Limnol. Oceanogr., 51(6), 2006, 2746–2762

Assessment of the processes controlling seasonal variations of dissolved inorganic carbon in the North Sea

Yann Bozec[1]
Royal Netherlands Institute for Sea Research, P.O. Box 59, NL-1790 AB Den Burg, The Netherlands

Helmuth Thomas
Canada Research Chair, Dalhousie University, Department of Oceanography, 1355 Oxford Street, Halifax, Nova Scotia B3H 4J1, Canada

Laure-Sophie Schiettecatte and Alberto V. Borges
Chemical Oceanography Unit, MARE, University of Liège, Institut de Physique (B5), B-4000, Liège, Belgium

Khalid Elkalay and Hein J. W. de Baar
Royal Netherlands Institute for Sea Research, P.O. Box 59, NL-1790 AB Den Burg, The Netherlands

Abstract

We used a seasonal North Sea data set comprising dissolved inorganic carbon (DIC), partial pressure of CO_2 (pCO_2), and inorganic nutrients to assess the abiotic and biological processes governing the monthly variations of DIC. During winter, advection and air–sea exchange of CO_2 control and increase the DIC content in the surface and deeper layers of the northern and central North Sea, with the atmosphere supplying CO_2 on the order of 0.2 mol C m^{-2} $month^{-1}$ to these areas. From February to July, net community production (NCP) controls the seasonal variations of DIC in the surface waters of the entire North Sea, with a net uptake ranging from 0.5 to 1.4 mol C m^{-2} $month^{-1}$. During the August–December period, NCP controls the seasonal variations of DIC in the southern North Sea, with a net release ranging from 0.5 to 0.8 mol C m^{-2} $month^{-1}$. Similarly, during the April–August period in the deeper layer of the northern North Sea, the NCP was the main factor controlling DIC concentrations, with a net release ranging from 0.5 to 5.5 mol C m^{-2} $month^{-1}$. In the surface layer of the North Sea, NCP on the basis of DIC was 4.3 ± 0.4 mol C m^{-2} yr^{-1}, whereas, NCP on the basis of nitrate was 1.6 ± 0.2 mol C m^{-2} yr^{-1}. Under nutrient-depleted conditions, preferential recycling (extracellular) of nutrients and intracellular mechanisms occurred and were responsible for the non-Redfield uptake of DIC versus nitrate and phosphate.

Coastal and marginal seas play a key role in the global carbon cycle by linking terrestrial, oceanic, and atmospheric reservoirs (Walsh 1991; Mackenzie et al. 2004). They occupy only 7% of the global ocean surface area but house 10–30% of the global marine primary production (Gattuso et al. 1998). Recent investigations have underlined the importance of coastal seas in the global carbon cycle and the necessity of introducing them into realistic models, notably to quantify the air–sea exchange of CO_2 (Chen 2004; Thomas et al. 2004; Muller-Karger et al. 2005). However, even the latest global estimates of the oceanic uptake of anthropogenic CO_2 (Sabine et al. 2004) do not include coastal seas in the calculations because of the small-scale variability observed within each marginal sea and between all marginal seas worldwide and because of the difficulty in increasing the spatial resolution of global numerical models.

Despite growing interest and debate on the role of all coastal seas in the global carbon cycle, robust estimates of the CO_2 air–sea fluxes are only available for a few individual coastal ecosystems. The air–sea exchange of CO_2 has been more intensively investigated in temperate marginal seas. Marginal seas account for a relatively large portion of the CO_2 uptake of the entire coastal ocean because they cover 55.6% of the total surface area of the coastal ocean (*see* for overview Borges 2005; Borges et al. 2005; Bozec et al. 2005). The links between air–sea exchange of CO_2, biological processes, and physical forcing have also been investigated to determine the net community production (NCP) in coastal seas and open shelves, notably for the Baltic Sea and Bering Chukchi sea shelf (Thomas

[1] To whom correspondence should be addressed. Present address: Scripps Institution of Oceanography, Geophysical Research Division, 9500 Gilman Drive, University of California San Diego, La Jolla, California 92093-0244 (ybozec@ucsd.edu).

Acknowledgments

We thank the captains and crews of RV *Pelagia* for their excellent cooperation during the cruises. The constructive comments by two anonymous reviewers, which helped improve the manuscript significantly, are gratefully acknowledged.

This study has been supported by the Netherlands Organization for Scientific Research (NWO), grants 810.33.004 and 014.27.001; the Dutch–German bilateral cooperation NEBROC; and the Belgium Federal Office for Scientific, Technical, and Cultural Affairs (CANOPY project, EV/03/20).

This study has been encouraged by and contributes to the LOICZ core project of the IGBP and to CARBO-OCEAN, an integrated project of the European Union (contract 511176-2).

and Schneider 1999; Osterroht and Thomas 2000; Kaltin and Anderson 2004). Similar investigations have been carried out in adjacent areas of the North Sea, such as the Norwegian Sea and the Nordic Seas (Falck and Gade 1999; Falck and Anderson 2005). Moreover, the link between the trophic state of the coastal seas and the air–sea exchange of CO_2 has recently been discussed. Heterotrophic systems do not necessarily release CO_2 to the atmosphere, and autotrophic systems do not necessarily act as sinks of atmospheric CO_2 (Borges 2005; Thomas et al. 2005*a*).

The North Sea is among the best studied coastal areas worldwide with respect to its physical, chemical, and biological conditions because it has been subject to detailed investigations for many decades. Earlier carbon cycle studies in the North Sea were confined to certain nearshore coastal areas such as the German Bight, the Wadden Sea, or the Belgian coast (*see* for overview Bozec et al. 2005). Recently, an intense field study showed that the North Sea is a sink of CO_2 for the atmosphere and absorbs 1.4 mol C m^{-2} yr^{-1} (Thomas et al. 2004). Moreover, Bozec et al. (2005) underlined the importance of the late summer season on the annual air–sea fluxes of CO_2 and confirmed the importance of the regional variability in the carbon cycle in the North Sea.

In this paper, we combined a comprehensive data set of dissolved inorganic carbon (DIC) and partial pressure of CO_2 (pCO_2) on the basis of four consecutive cruises in the North Sea with data on water flux. The goal of this study is to identify and quantify the biological and physical processes responsible for the seasonal variations of DIC in the North Sea. Moreover, the assessment of these different processes allows us to compute the NCP of carbon in the North Sea directly on the basis of the DIC data set covering the four seasons of the year. NCP was computed by mass balances of DIC and of inorganic nutrients (nitrate and phosphate) according to the International Council for the Exploration of the Sea (ICES) boxes, and the water fluxes were computed by European Regional Seas Ecosystem Model (ERSEM; Lenhart et al. 1995; Lenhart and Pohlmann 1997).

Material and methods

Sampling and analytical measurement—Data were obtained during four cruises in the North Sea (18 Aug 2001–13 Sep 2001, 06 Nov 2001–29 Nov 2001, 11 Feb 2002–05 Mar 2002, and 06 May 2002–26 May 2002) on board RV *Pelagia*. The North Sea was covered during summer, fall, winter, and spring by an adapted $1^\circ \times 1^\circ$ grid with 97 stations (Fig. 1). This grid was specifically designed to focus on the relevant regions for biogeochemical cycles such as the Shetland and English Channels (inflow of North Atlantic water), the Skagerrak area (inflow of Baltic Sea water), and the western Scandinavian coast (outflow to the North Atlantic). The stations were also denser in the Southern Bight (Fig. 1), which receives the major freshwater inputs, whereas station distribution was sparser in the more homogeneous central North Sea.

During each cruise, a total of ~750 water samples was collected for DIC; dissolved oxygen (O_2); the inorganic

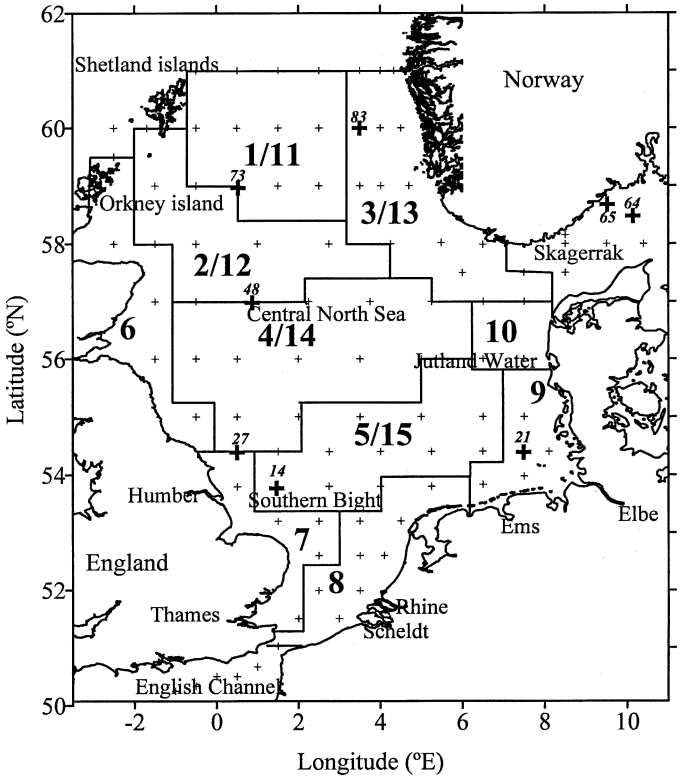

Fig. 1. Map of the study area and the International Commission for the Exploration of the Seas (ICES) boxes. Boxes 1–5 represent the first 30 m of the water column, whereas boxes 11–15, below boxes 1–5, represent the bottom layer of the water column. The other boxes (6–10) are one-layer boxes representing the whole water column. Crosses represent the stations sampled during the four cruises. Bold crosses with italic numbers correspond to the stations for which the profiles are shown in Fig. 3.

nutrients nitrate (NO_3^-), nitrite (NO_2^-), and phosphate (PO_4^{3-}); chlorophyll *a* (Chl *a*; in surface waters during spring and summer); salinity; and temperature. In the surface waters, salinity, temperature, and pCO_2 were determined continuously from the ship's water supply, yielding 22,000 surface measurements per cruise for these variables (Thomas et al. 2004; Bozec et al. 2005).

For the detailed description of the sampling and analytical techniques of DIC and pCO_2, please refer to Bozec et al. (2005) and Thomas (2002). NO_3^-, NO_2^-, and PO_4^{3-} were analyzed within 10 h of sampling with a Technicon TRAACS 800 auto-analyzer according to Grasshoff et al. (1983). The standard deviation for the sum of NO_3^- and NO_2^- (NO_x) was ± 0.02 μmol L^{-1} and for PO_4^{3-} was ± 0.01 μmol L^{-1}. The estimated accuracies were $\pm 1.5\%$ and 3% for NO_x and PO_4^{3-}, respectively. The concentration of Chl *a* was determined from GF/F-filtered samples by the fluorimetric method according to the method of Holm-Hansen et al. (1965) with a precision of $\pm 4\%$.

Calculation of the different parameters influencing the variability of DIC—The study area was divided into sets of

Table 1. The 10-yr (1982–1992) mean net water flow across the boundaries of the North Sea with the Atlantic Ocean and Baltic Sea from Lenhart et al. (1995). Positive values indicate inputs into the North Sea and negative values are outputs from the North Sea. These flows are calculated for different boxes (i.e., different areas and layers of the North Sea). The net inflow from the Baltic Sea (264 km^3 $month^{-1}$) into boxes 3/13 is overestimated by a factor of three to four (Thomas et al. 2005*a*).

Box	Atlantic Ocean inflow/outflow (km^3 $month^{-1}$)	Baltic Sea inflow/outflow (km^3 $month^{-1}$)
1	751	—
2	212	—
3	−681	−389
6	697	—
8	148	—
11	2,476	—
12	246	—
13	−4,113	653

surface (1–5) and deep (11–15) boxes in the stratified central and northern North Sea (region 1) and five single boxes (6–10) in the single-layered southern North Sea (region 2; ICES 1983; Fig. 1). The boxes have different surface areas and depths, except for surface boxes 1–5, all with a depth of 30 m. Region 1 covers an area of 336,518 km^2, and the upper and bottom layers have a water volume of 6,485 km^3 and 27,279 km^3, respectively. Region 2 covers an area of 176,486 km^2 with a water volume of 6,643 km^3. Horizontal and vertical advection between the boxes, the air–sea CO_2 exchange with the surface boxes (1–10), and the net biological term are considered the main factors controlling the distribution of DIC in each box of the North Sea. The freshwater DIC input into boxes 7, 8, and 9 by rivers yields three additional DIC advection terms. The DIC input into box 3 from fjords is assessed by the monthly salinity changes within box 3.

Advection term: We used the 10-yr (1982–1992) mean net water mass transports for the above ICES boxes (ICES 1983) as reported by Lenhart et al. (1995; Table 1) to compute the monthly variations in DIC for each box from horizontal and vertical advection (ΔDIC_{adv}). For each cruise, we calculated the specific DIC (water column inventory of DIC divided by the water column depth) at each station for the upper layer (30 m) and bottom layer (below 30 m) of the water column and averaged these for the individual boxes. Accordingly, the DIC concentrations calculated for each box and season rely on 12–60 measurements, depending on the number of stations per box and the vertical resolution of sampling in the water column. Because the mean flushing time for every box is on the order of 30–40 d (Lenhart et al. 1995), we assumed that the specific DIC calculated per box is representative of the whole month. The limit of 30 m has been chosen in ERSEM because it is the average depth of the thermocline in the area in which stratification occurs in the North Sea and is the boundary between boxes 1 and 11, 2 and 12, 3 and 13, 4 and 14, and 5 and 15 (Fig. 1; Lenhart et al. 1995).

Freshwater inputs: The advection term takes into account the lateral and vertical flows between all the boxes. However, for several boxes that receive high freshwater inputs with different DIC concentrations, it is necessary to quantify the effects of these inputs on the DIC variations.

The coastal boxes (6–9) receive high freshwater inputs from the Humber, Thames, Scheldt, Rhine, Ems, and Elbe estuaries. We introduced the annual integrated fluxes out of the estuaries calculated by A. V. Borges (unpubl.) into the relevant boxes, taking into account the seasonal variations of these fluxes. For these boxes, the advection term ΔDIC_{adv} represents the variations in DIC concentration from the lateral and vertical advection and from the DIC fluxes from the estuaries.

For box 3, which receives high freshwater inputs with low DIC concentrations from the Scandinavian coast, a term for the monthly variations of DIC because of freshwater inflow (ΔDIC_{fw}) has been introduced. We calculated the difference in DIC concentration (ΔDIC) between the summer and the fall cruises and the concomitant difference in salinity (ΔS) for the stations of box 3 influenced by these freshwater inputs. The plot of ΔDIC versus ΔS showed a linear relationship between these two parameters for the stations of box 3 situated along the Norwegian coast ($\Delta DIC_{fw} = 28.8\Delta S - 71.5$; $r^2 = 0.9$, $n = 10$). The slope of this linear regression represents the changes in DIC as a result of freshwater inputs into box 3 for the summer–fall period. Similar trends could be established for the fall–winter ($\Delta DIC_{fw} = 21.6\Delta S - 27.8$; $r^2 = 0.8$, $n = 12$), winter–spring ($\Delta DIC_{fw} = 16.7\Delta S - 31.5$; $r^2 = 0.9$, $n = 12$), and spring–summer ($\Delta DIC_{fw} = 18.5\Delta S - 104.1$; $r^2 = 0.7$, $n = 10$) periods. The monthly changes in DIC because of the freshwater inputs into box 3 were -10 mmol m^{-3} from summer to fall (salinity decreased by 0.40), +7 mmol m^{-3} from fall to winter (increase in salinity of 0.78), -6 mmol m^{-3} from winter to spring (decrease in salinity of 2.01), and +7 mmol m^{-3} from spring to summer (increase in salinity of 1.60).

The air–sea exchange term: The flux of CO_2 at the air–sea interface was recalculated from the pCO_2 dataset of Thomas et al. (2004) for the ICES boxes with the use of wind speed data provided by the European Centre for Medium-Range Weather Forecast (ECMWF) and the gas transfer velocity (k) parameterization of Wanninkhof and McGillis (1999), hereafter referred to as W&McG99. We calculated a monthly average value of these fluxes for each box every month. Once integrated over the upper part of the water column, these fluxes represent the monthly changes in DIC because of air–sea CO_2 exchange ($\Delta DIC_{air-sea}$). Because the biological term (*see* the section *The biological term* below) is very dependent on the choice of the gas transfer velocity constant, the effects of two different k-wind speed formulations (Wanninkhof 1992; Nightingale et al. 2000), hereafter referred to as W92 and N2000, respectively, on the calculation of the various DIC fluxes are discussed in the section *Robustness of the* NCP_C *calculation*.

The diffusion term: The vertical diffusive fluxes of DIC (F_d) from the deeper layer into the upper layer of the water column through the halocline of the northern boxes (1/11–5/15) were calculated by Fick's law,

$$F_d = K_v \times dc/dx \quad (1)$$

where K_v is the eddy diffusive coefficient and dc/dx represents the gradient of DIC at the boundary between the halocline and the bottom layer. The diffusion coefficients of Lenhart et al. (1995) given for each month were used. These coefficients varied from 50 to 600 $cm^2\ s^{-1}$ from summer to winter, respectively, and are on the same order as the value of 300 $cm^2\ s^{-1}$ in the Baltic Sea calculated by Osterroht and Thomas (2000). The diffusive fluxes were negligible for the whole year because the highest values of K_v in winter were associated with a very small DIC gradient, whereas when the strongest DIC gradients were present in summer, the values of K_V were close to zero.

The biological term: We linearly interpolated the seasonal specific DIC variations between the observed values in each box and calculated the observed DIC variation between two successive months (ΔDIC_{obs}) for the whole year. For all the boxes, Eq. 2 expresses ΔDIC_{obs} as a function of the relevant parameters for the DIC monthly variability.

$$\Delta DIC_{obs} = \Delta DIC_{bio} + \Delta DIC_{air-sea} + \Delta DIC_{adv} \quad (2)$$

Moreover, for box 3, the equation is extended,

$$\Delta DIC_{obs} = \Delta DIC_{bio} + \Delta DIC_{air-sea} + \Delta DIC_{adv} + \Delta DIC_{fw} \quad (3)$$

by the freshwater effect for DIC input by fjords. The net effect of the overall biological processes on the monthly variations of DIC can be calculated with Eq. 4 (Eq. 5 for box 3).

$$\Delta DIC_{bio} = \Delta DIC_{obs} - (\Delta DIC_{air-sea} + \Delta DIC_{adv}) \quad (4)$$

$$\Delta DIC_{bio} = \Delta DIC_{obs} - (\Delta DIC_{air-sea} + \Delta DIC_{adv} + \Delta DIC_{fw}) \quad (5)$$

The obtained term, ΔDIC_{bio}, is an overall term inherently comprising photosynthesis, respiration, biocalcification, and $CaCO_3$ dissolution and exchanges of carbon with surface sediments. Within each box, the net balance of photosynthesis and respiration yields monthly changes of the inventory of biogenic suspended particulate (POC) and dissolved organic carbon (DOC). ΔDIC_{bio} in the deeper boxes includes pelagic organic matter respiration but also inherently considers carbon exchanges with the surface sediments. These carbon fluxes are caused by respiration of organic matter, which had settled temporarily onto the surface sediments. Long term, net carbon burial does not occur in the North Sea, except for a trivial net burial in box 13, which accounts for only <1% of all primary production of the whole North Sea (de Haas et al. 2002) and is deemed to be negligible on an annual scale for our purposes. In other words, neither box 13 nor other bottom boxes 6–12, 14, or 15 have a burial loss term.

Production/dissolution of calcium carbonate: Ecosystem calcification has not been considered in a number of recent papers on carbon and nutrient cycles of the North Sea because it is not perceived to be a significant component of the carbon cycle compared with the three main factors above. Blooms of the calcifying cocolithophores *Emilia huxleyi* have only been reported in the northern part of the North Sea (Tyrell and Merico 2004 and references therein), where the stratification of the water column is favorable for the occurrence of these blooms. Because of the high spatial and temporal variability in the occurrence of these blooms, it is difficult to quantify their effect on monthly DIC variations. Most of the coccolithophore blooms occur during the June–July period in boxes 1, 2, and 3, although blooms can also occur in fall. For the northern North Sea, the term ΔDIC_{bio} comprises the changes in DIC from pelagic calcification and dissolution of $CaCO_3$. As far as the southern North Sea is concerned, to the best of our knowledge, blooms of calcifying pelagic species such as coccolithophores have not been reported (Tyrell and Merico 2004). The absence of stratification and the homogeneous shallow water column limit incoming light, resulting in unfavorable conditions for the occurrence of these blooms (Tyrell and Merico 2004).

Robustness of the NCP calculations—NCP is defined as the difference between gross primary production (GPP) and community respiration (R). In autotrophic systems, production of organic matter is larger than its consumption (GPP > R) and excess organic matter is stored, exported, or both. In heterotrophic systems, decomposition of organic matter predominates (R > GPP), and such systems must therefore be supported by external inputs of organic matter (Odum 1956).

We calculated net community production on the basis of ΔDIC_{bio} values (NCP_C) for each ICES box, the 30-m depth of the upper boxes, and the maximum depth of each one-layer box. For the NCP_C computations, we relied on numerous stations with a high vertical resolution for each cruise (each season). The DIC values attributed to each box were representative of the area studied at the time of the cruise because the flushing times of the boxes are on the order of 30 d.

The air–sea CO_2 fluxes computed from two recent parameterizations (W&McG99 and N2000, the latter established in the southern North Sea) were very similar and did not significantly change the NCP_C estimates (seasonal and annual integrated values). The W92 parameterization would decrease the annual NCP_C for the whole North Sea by 3% and the NCP_C calculated for the productive period (February–July) by 10% compared with the results from the W&McG99 parameterization. We used the W&McG99 parameterization for a direct comparison with the results of Thomas et al. (2004). Here, the calculation of NCP_C is relatively insensitive to the choice of gas transfer velocity, as also shown in other coastal ecosystems characterized by relatively low air–sea CO_2

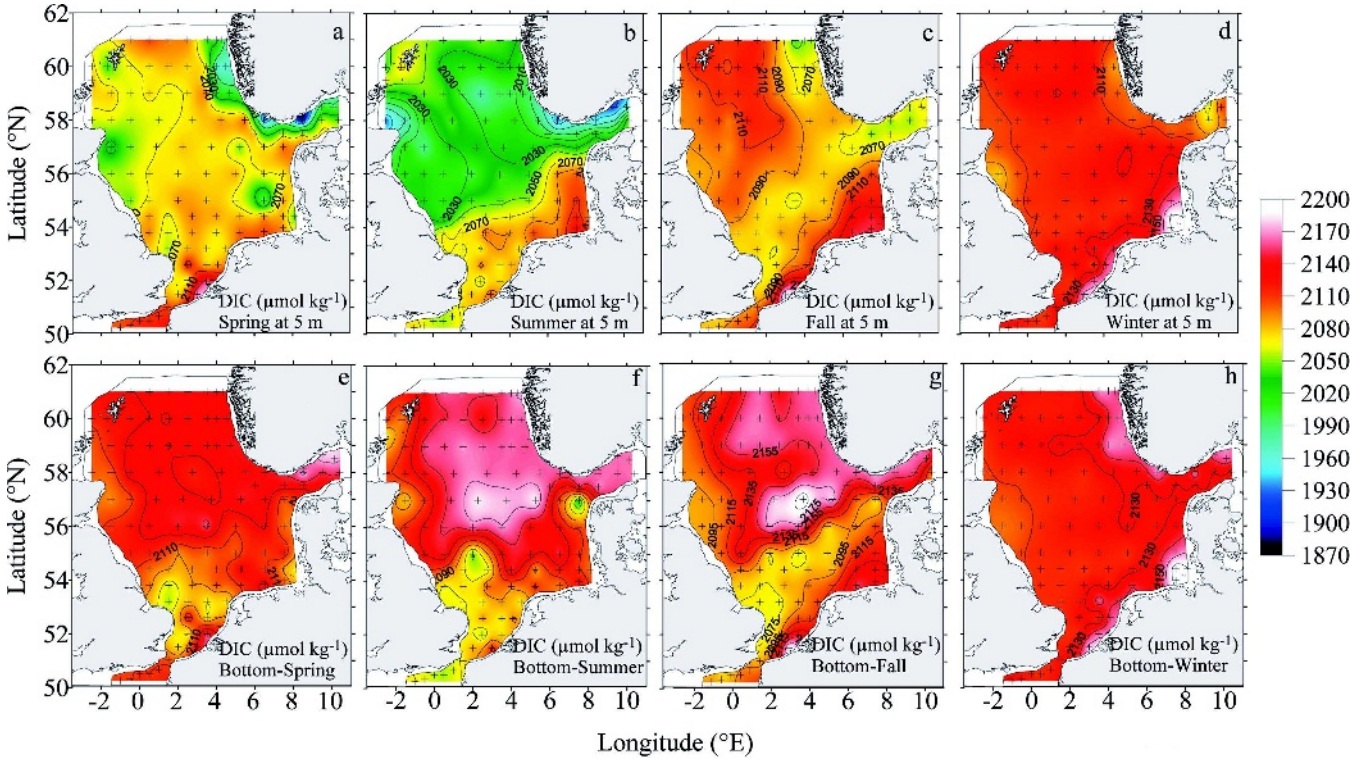

Fig. 2. Horizontal distribution of DIC concentrations (μmol kg^{-1}) for the (a) spring, (b) summer, (c) fall, and (d) winter surface waters (5 m depth). Horizontal distribution of DIC concentrations (μmol kg^{-1}) for the (e) spring, (f) summer, (g) fall, and (h) winter in bottom waters.

fluxes (Gazeau et al. 2005*a*). In ecosystems characterized by very large air–water CO_2 fluxes such as estuaries, the air–sea exchange term can be very significant in the NCP computations (Gazeau et al. 2005*b*).

We have used the average values of the advection term calculated for the years 1982–1992 given by Lenhart et al. (1995). Lenhart and Pohlmann (1997) showed that the interannual variations for these flows are minor. Because the meteorological conditions observed for the years 2001 and 2002 were similar to the common climatological conditions in the North Sea, we can assume a similarity of the water flow estimates. Moreover, reducing the mixing term in one box by 50% would only affect our value for the annual NCP_C by 2% and the NCP_C for the productive period by 5%. Our NCP_C values calculated for the whole year and for the productive period in the North Sea are given with a range of uncertainty of $\pm$10% and $\pm$20%, respectively.

Results

DIC distribution—During spring, the surface DIC had a rather homogeneous distribution in the central North Sea with an average value of 2,085 μmol kg^{-1} (Fig. 2a). However, the inflow of North Atlantic water through the Shetland Channel in the northwestern part of the North Sea had lower concentrations of 2,070 μmol kg^{-1}. Lowest concentrations were found in the transition area between the North and Baltic Seas (Skagerrak) and along the southwestern coast of Norway, with concentrations as low as 1,870 μmol kg^{-1}. The plume of the Scheldt River was marked by the highest concentration of 2,150 μmol kg^{-1}.

Bozec et al. (2005) investigated the surface distribution of DIC in late summer in detail. In short, the DIC distribution showed a clear boundary at ~54°N, with higher concentrations in the southern area ranging from 2,090 to 2,130 μmol kg^{-1} compared with the central North Sea (values between 1,980 and 2,070 μmol kg^{-1}; Fig. 2b). The Skagerrak area had the lowest values, between 1,870 and 2,030 μmol kg^{-1}.

In fall, increased wind speed induced mixing between the upper and bottom layers of the water column, as well as a lateral mixing, which increased the surface concentrations of DIC almost in the whole North Sea (Fig. 2c). Concentrations in the Skagerrak and along the southwestern coast of Norway were 2,070 μmol kg^{-1}, whereas along the Danish, German, Dutch, and Belgium coasts, DIC concentrations were close to 2,110 μmol kg^{-1}. Values in the rest of the North Sea ranged between 2,090 and 2,110 μmol kg^{-1}.

In winter, the surface water of the whole North Sea had a homogeneous DIC concentration of 2,120 μmol kg^{-1} (Fig. 2d), mainly because of vertical and horizontal mixing of water masses. Only at the stations in the front of the Elbe and Scheldt estuaries in the southern area were DIC concentrations higher than in the rest of the North Sea, with values as high as 2,150 μmol kg^{-1}. Again, in the Skagerrak area and along the southwestern coast of Norway, concentrations of DIC were lower with values of 2,090 μmol kg^{-1}.

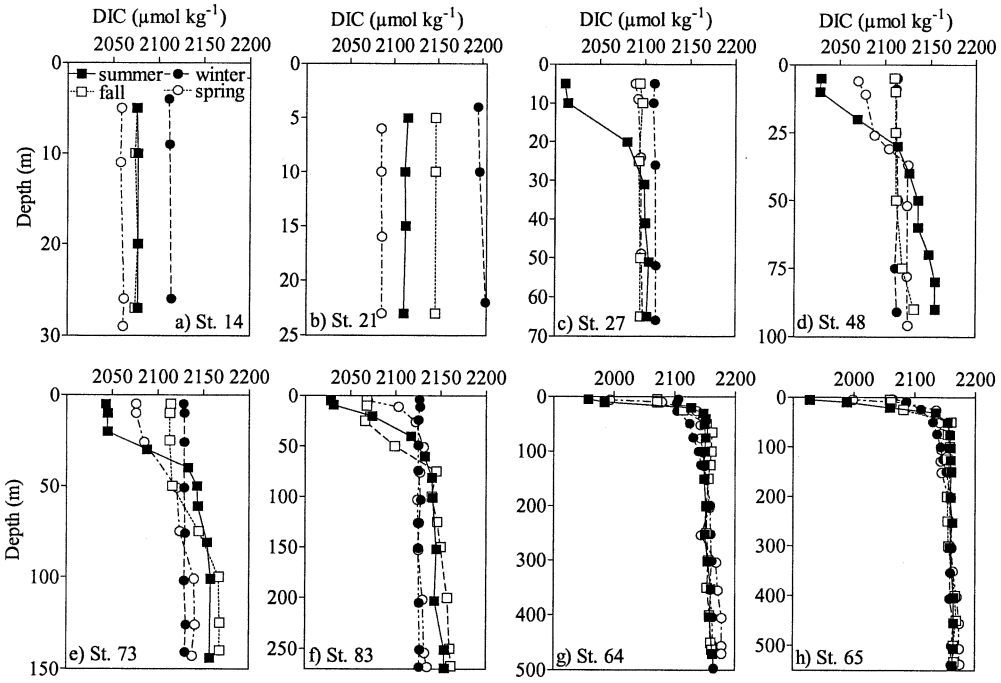

Fig. 3. Profiles of the vertical seasonal variations of DIC concentrations from the CTD data for eight stations situated in the specific regions of the North Sea: Stas. (a) 14, (b) 21, (c) 27, (d) 48, (e) 73, (f) 83, (g) 64, and (h) 65. The positions of the stations are indicated on Fig. 1.

It is difficult to compare the DIC concentrations in the deeper layer of the North Sea because bottom depths range approximately from 20 to 700 m. We therefore discuss the maps of DIC concentrations in the bottom of the North Sea and present several profiles representative of the different water column properties encountered in the North Sea. Figure 2 shows that surface and bottom DIC concentrations of the southern area (south of ~54°N), where depths range from 20 to 60 m, were very similar throughout the year. This is a direct consequence of the water column in this area being mixed down to the bottom for most of the year (Fig. 3a,b). However, in spring, at the deepest stations (40–60 m), as well as in the German Bight, the water column was stratified (Fig. 3c) and DIC concentrations were lower in the upper layer (2,080 μmol kg^{-1}) than in the bottom layer (2,110 μmol kg^{-1}; compare Fig. 2a,e).

In the deeper layers of the northern North Sea, from spring to summer and from summer to fall, we observed increasing DIC concentrations from 2,135 μmol kg^{-1} (spring) to 2,155 μmol kg^{-1} (summer) and a maximum of 2,175 μmol kg^{-1} (fall; Fig. 2e–g). This is also evident from profiles recorded in the central and northern North Sea at several stations; for example, at Stas. 48, 73, and 83 (Fig. 3d–f), a clear increase was observed below the thermocline from spring to summer and from summer to fall.

At the very deep stations situated in the Skagerrak area, the bottom DIC concentrations were very similar throughout the year. For Stas. 64 and 65 (Fig. 3g,h), the DIC concentrations from 300 to 500 m were constant, with values of ~2,150 μmol kg^{-1}, as also seen on the bottom map of DIC in the Skagerrak area (Fig. 2). However, at these stations between 50 and 200 m (similar to the shallower stations of the central North Sea), DIC concentrations were much higher during summer and fall (2,165 μmol kg^{-1}) than during winter or spring (2,120 μmol kg^{-1}). This suggests that the respiration of organic matter occurred just below the thermocline and increased the DIC concentrations, whereas in the deeper part of the water column, the effect of respiration is not evident from the DIC measurements.

Tables 2 and 3 summarize the surface water characteristics of the CO_2 system and ancillary data measured during the four cruises in the ICES boxes. A detailed description of the spatial and temporal variability of pCO_2 is provided by Thomas et al. (2004, 2005*b*).

Seasonal variations of ΔDIC_{bio}, ΔDIC_{adv}, and $\Delta DIC_{air-sea}$ in region 1—The results of the DIC mass balance computations for region 1 are shown in Fig. 4 for boxes 1/11, which are representative of the northern North Sea, and Fig. 5 for boxes 4/14, which are representative of the central North Sea. Tables 4 and 5 gather the data for all the boxes of region 1. For the surface boxes of this region, biological processes were the main factors controlling the DIC concentrations from February to August and decreased the DIC concentrations (revealing GPP > R) with maximum values for ΔDIC_{bio} observed in April in box 5 and in May for the other boxes (Tables 4, 5). This strong uptake of DIC was accompanied by an uptake of CO_2 from the atmosphere to the surface layer, which was responsible for an increase in DIC concentrations of ~10 mmol m^{-3} during the whole period. Values of ΔDIC_{adv} were positive

Table 2. Range of values observed for the main parameters measured during the four cruises in the upper layer of the stratified ICES boxes. For DIC, NO_x, PO_4^{3-}, and Chl *a*, values were taken from station data, whereas for temperature (Temp), salinity, and pCO_2, values were taken from continuous measurements made in each box.

Box	Season	Salinity	Temp (°C)	DIC (μmol kg^{-1})	pCO_2 (μatm)	NO_x (μmol L^{-1})	PO_4^{3-} (μmol L^{-1})	Chl *a* (μg L^{-1})
1	Summer	34.20–35.25	12.80–17.70	1,979–2,059	260–300	0.00–0.35	0.00–0.11	0.23–3.31
	Fall	33.38–35.28	8.90–10.40	2,088–2,120	301–356	4.86–8.69	0.33–0.59	—
	Winter	35.15–35.35	7.35–9.26	2,117–2,131	340–365	8.47–10.87	0.59–0.73	—
	Spring	33.94–35.38	8.76–9.54	2,063–2,107	254–338	0.10–6.87	0.07–0.52	0.67–4.01
2	Summer	34.67–35.02	12.70–15.70	1,968–2,043	220–340	0.00–1.84	0.01–0.31	0.22–2.85
	Fall	34.83–35.08	9.30–10.80	2,098–2,119	337–357	4.19–7.36	0.35–0.53	—
	Winter	34.76–35.11	7.12–8.03	2,105–2,118	339–354	7.11–8.62	0.55–0.62	—
	Spring	34.59–35.12	8.56–9.42	2,047–2,081	260–298	0.03–1.73	0.07–0.22	0.21–4.96
3	Summer	30.46–34.75	13.70–17.80	1,935–2,031	240–310	0.01–0.20	0.00–0.04	0.27–0.92
	Fall	31.80–33.75	9.20–11.60	2,039–2,089	302–358	2.38–4.14	0.20–0.38	—
	Winter	32.38–35.30	5.12–8.61	2,089–2,126	339–368	7.26–18.01	0.52–1.13	—
	Spring	22.73–35.09	7.69–10.02	1,927–2,100	256–340	0.03–4.99	0.04–0.79	0.59–3.06
4	Summer	34.58–35.02	15.40–16.50	1,995–2,040	220–380	0.00–0.17	0.01–0.03	0.26–1.05
	Fall	34.36–34.92	9.00–11.00	2,072–2,105	298–373	1.75–4.79	0.18–0.44	—
	Winter	34.60–35.00	5.90–7.71	2,104–2,131	339–366	6.04–8.00	0.55–0.68	—
	Spring	34.62–34.95	9.00–10.12	2,045–2,081	242–306	0.06–0.18	0.07–0.15	0.21–2.46
5	Summer	33.11–34.79	14.50–18.40	2,044–2,100	340–460	0.00–0.52	0.01–0.26	0.22–1.72
	Fall	33.30–34.79	10.10–12.90	2,061–2,133	304–360	0.12–7.84	0.17–0.52	—
	Winter	34.07–34.84	5.98–6.89	2,111–2,133	332–375	3.96–13.24	0.40–0.68	—
	Spring	33.51–34.76	9.76–12.01	2,059–2,095	190–351	0.00–3.63	0.02–0.12	0.13–1.76

because the advection was mostly due to vertical influx of deeper water with higher DIC content. The effect of advection was higher in the deeper areas (boxes 1, 2, and 3) because of the stronger gradient of DIC in the water column (*compare* Fig. 3c,e) and was ~10 mmol m^{-3} in spring and 15 mmol m^{-3} in summer when the DIC gradient was more pronounced (Tables 4, 5).

For the period from August to November, ΔDIC_{adv} was the main factor increasing the surface DIC concentrations in box 1 with values of 10 mmol m^{-3}. During this season, the surface waters of the northern North Sea were still undersaturated in CO_2 compared with the atmosphere, which, associated with higher wind speeds, caused an influx of CO_2 responsible for an increase of DIC concentrations in the surface waters of 5–10 mmol m^{-3}.

From November to January, no significant variations in the DIC surface concentrations were observed in box 1. At this time of the year, the water column was mixed down to

Table 3. Range of values observed for the main parameters measured during the four cruises for the one-layer ICES boxes. For DIC, NO_x, PO_4^{3-}, and Chl *a*, values were taken from the station data, whereas for temperature (Temp), salinity, and pCO_2, values were taken from the continuous measurements made for each box.

Box	Season	Salinity	Temp. (°C)	DIC (μmol kg^{-1})	pCO_2 (μatm)	NO_x (μmol L^{-1})	PO_4^{3-} (μmol L^{-1})	Chl *a* (μg L^{-1})
6	Summer	34.26–34.79	11.70–15.40	2,018–2,067	220–280	0.00–0.34	0.03–0.22	0.40–5.31
	Fall	34.35–34.95	10.00–11.00	2,084–2,101	348–370	3.77–6.46	0.45–0.50	—
	Winter	34.09–34.76	6.63–8.18	2,079–2,107	346–356	6.08–9.49	0.58–0.68	—
	Spring	34.31–34.99	8.69–9.11	2,020–2,084	238–307	0.05–1.21	0.06–0.20	1.85–1.98
7	Summer	33.95–34.36	13.80–18.20	2,066–2,096	300–460	1.15–2.18	0.17–0.25	0.45–1.51
	Fall	34.32–34.57	11.20–12.80	2,068–2,085	345–375	2.40–6.55	0.25–0.51	—
	Winter	33.92–34.92	6.21–8.93	2,111–2,131	352–369	7.62–14.48	0.43–0.81	—
	Spring	34.01–35.01	9.58–12.47	2,054–2,122	290–390	0.03–13.42	0.02–0.46	0.79–7.15
8	Summer	32.88–34.36	17.40–19.00	2,059–2,099	340–430	0.07–2.10	0.02–0.45	0.54–5.55
	Fall	32.40–34.50	10.70–12.70	2,082–2,190	311–385	3.45–20.67	0.16–0.86	—
	Winter	33.36–34.91	6.59–8.90	2,103–2,177	302–371	7.28–23.31	0.18–0.72	—
	Spring	31.69–35.18	11.26–13.36	2,067–2,171	262–372	0.15–13.22	0.01–0.27	1.02–6.52
9	Summer	30.04–32.20	17.90–19.20	2,093–2,130	370–450	0.14–4.72	0.06–1.00	2.01–3.80
	Fall	28.49–32.98	8.08–11.20	2,119–2,162	338–425	5.91–37.89	0.53–1.39	—
	Winter	25.58–33.82	4.59–6.68	2,132–2,195	350–371	14.28–61.9	0.44–1.14	—
	Spring	28.88–32.78	10.60–12.75	2,040–2,091	206–335	9.10–25.10	0.01–0.07	2.11–3.58
10	Summer	32.26–33.45	17.10–17.30	2,091–2,101	290–380	0.04–0.37	0.02–0.13	1.05–1.50
	Fall	32.49–34.32	11.00–12.50	2,090–2,111	353–365	3.30–6.75	0.53–0.73	—
	Winter	33.58–34.36	5.55–6.19	2,122–2,137	348–366	8.49–13.74	0.53–0.60	—
	Spring	30.80–33.93	9.99–11.21	2,071–2,072	257–292	1.08–21.98	0.01–0.02	0.53–1.33

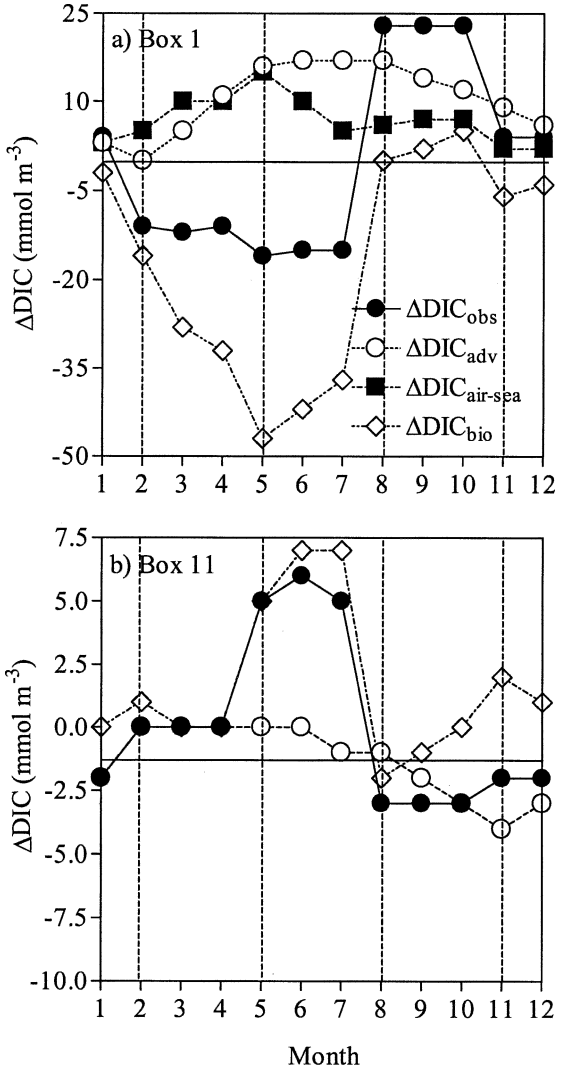

Fig. 4. Monthly effects of advection (ΔDIC_{adv}), air–sea CO_2 exchange ($\Delta DIC_{air-sea}$), and biological processes (ΔDIC_{bio}) on the variations of DIC (ΔDIC_{obs}) in the northern North Sea for stratified (a) box 1 and (b) box 11. The dotted vertical lines correspond to the cruises.

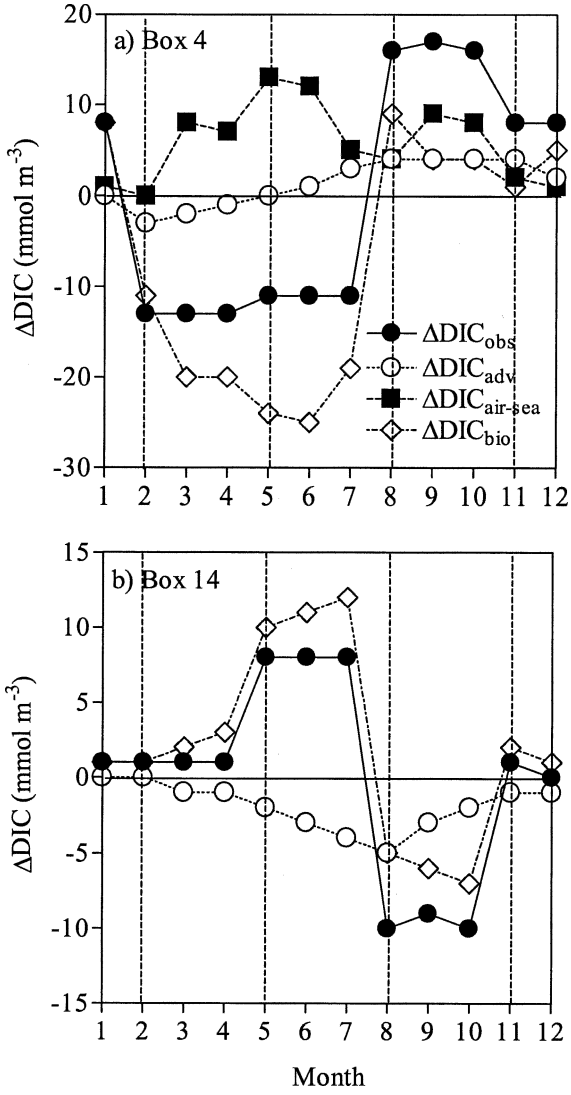

Fig. 5. Monthly effects of advection (ΔDIC_{adv}), air–sea CO_2 exchange ($\Delta DIC_{air-sea}$), and biological processes (ΔDIC_{bio}) on the variations of DIC (ΔDIC_{obs}) in the central North Sea for (a) box 4 and (b) box 14. The dotted vertical lines correspond to the cruises.

150 m (Fig. 3e,f), and the surface distribution of DIC was homogeneous (Fig. 2d), resulting in insignificant ΔDIC_{adv}. For this period, the positive values of ΔDIC_{bio} in box 5 (and to a minor extent in box 4) showed that R dominated GPP and increase the DIC concentrations by 5 to 8 mmol m^{-3}.

For most of the deeper boxes of region 1, DIC concentrations did not vary significantly from November to May. For the period from April to August, positive values of ΔDIC_{bio}, ranging from 5 to 10 mmol m^{-3}, showed that R > GPP governs the DIC variation in the deeper part of region 1. The comparison of ΔDIC_{bio} in the upper and deeper layers of the stratified boxes (Fig. 6a) shows that degradation of organic matter occurred in the bottom layer between 2 and 3 months after the productive period started in the upper layer. This important result confirms that part of the organic material produced during spring and early summer in the upper layers is respired in the bottom layer, as also suggested by Bozec et al. (2005).

Seasonal variations of ΔDIC_{bio}, ΔDIC_{adv}, and $\Delta DIC_{air-sea}$ in region 2—Figure 7 shows the relative importance of biology, advection, and air–sea CO_2 exchange on the monthly DIC variations for two representative one-layer boxes. Table 6 gathers the results of the calculation for all one-layer boxes. From February to August, ΔDIC_{bio} values of −5 to −27 mmol m^{-3} show that GPP > R governed the DIC pool in region 2. These negative ΔDIC_{bio} values were associated with positive values of $\Delta DIC_{air-sea}$ in all the boxes, with the highest fluxes calculated for box 6 (Fig. 7a; Table 6).

On one hand, for the August–November period, the input of CO_2 from the atmosphere was the main factor governing DIC variations in the deepest one-layer box 6.

Table 4. The monthly DIC variations observed (ΔDIC_{obs}) in every box of the northern North Sea and the calculated changes attributable to advection (ΔDIC_{adv}), air–sea exchange ($\Delta DIC_{air-sea}$), biology (ΔDIC_{bio}), and freshwater inputs (ΔDIC_{fw}).

		DIC (mmol C m^{-3} $month^{-1}$)											
Box		Jan	Feb	Mar	Apr	May	Jun	Jul	Aug	Sep	Oct	Nov	Dec
1	ΔDIC_{obs}	4	−11	−12	−11	−16	−15	−15	23	23	23	4	4
	ΔDIC_{adv}	3	0	5	11	16	17	17	17	14	12	9	6
	$\Delta DIC_{air-sea}$	3	5	10	10	15	10	5	6	7	7	2	2
	ΔDIC_{bio}	−2	−16	−28	−32	−47	−42	−37	0	2	5	−6	−4
11	ΔDIC_{obs}	−2	0	0	0	5	6	5	−3	−3	−3	−2	−2
	ΔDIC_{adv}	−2	0	0	0	0	0	−1	−1	−2	−3	−4	−3
	ΔDIC_{bio}	0	1	0	0	5	7	7	−2	−1	0	2	1
2	ΔDIC_{obs}	3	−14	−14	−14	−11	−10	−11	22	22	22	3	2
	ΔDIC_{adv}	0	0	5	9	14	15	17	19	12	5	−2	−1
	$\Delta DIC_{air-sea}$	1	2	11	9	15	13	4	5	8	5	2	0
	ΔDIC_{bio}	2	−17	−30	−32	−39	−38	−32	−2	2	12	2	3
12	ΔDIC_{obs}	0	0	0	0	7	8	7	−7	−7	−7	−1	−1
	ΔDIC_{adv}	0	0	0	−1	−1	−3	−4	−5	−4	−2	−1	−1
	ΔDIC_{bio}	0	0	1	1	9	10	11	−2	−3	−5	0	0
3	ΔDIC_{obs}	14	−16	−16	−16	−6	−6	−6	7	7	8	15	15
	ΔDIC_{adv}	22	13	18	23	29	21	14	—	—	—	—	—
	$\Delta DIC_{air-sea}$	2	1	6	5	9	6	5	3	5	7	5	3
	ΔDIC_{bio}	−18	−24	−34	−38	−51	−41	−32	—	—	—	—	—
	ΔDIC_{fw}	7	−6	−6	−6	7	7	7	−10	−10	−10	7	7
13	ΔDIC_{obs}	−1	0	1	0	7	7	7	−6	−6	−6	−1	−1
	ΔDIC_{adv}	−5	−4	−5	−6	−6	−8	−9	−10	−9	−7	−5	−5
	ΔDIC_{bio}	4	4	6	6	13	14	16	4	3	1	4	4

During this period of the year, surface waters in box 6 were still undersaturated in CO_2 with respect to the atmosphere (Thomas et al. 2004), and the higher wind speeds enhanced the air–sea CO_2 exchange, with $\Delta DIC_{air-sea}$ ranging between 5 and 9 mmol m^{-3}. On the other hand, in the very shallow boxes 8 and 9, R > GPP governed the DIC variations from August to February, with ΔDIC_{bio} ranging between 5 and 15 mmol m^{-3}. This was concomitant with a release of CO_2 to the atmosphere, which decreased the DIC concentrations in the surface layer by 5 mmol m^{-3} in box 8 (Fig. 7b; Table 6). Results from Table 6 show that similar processes govern the DIC variations in box 7 from mid-October until February.

In region 1, GPP > R was observed in the upper layer, whereas predominant degradation of organic matter was observed in the bottom boxes with a delay of 2 to 3 months. In region 2, the degradation of organic matter largely predominates from August to January (Fig. 6b). This predominant degradation of organic matter is responsible for the higher DIC and pCO_2 values during late summer in the southern area, leading to a source of CO_2 to the atmosphere of 0.8–1.4 mmol m^{-2} d^{-1} for this area (Bozec et al. 2005).

Net community production of carbon—From February to July, the upper layer of region 1 was clearly autotrophic,

Table 5. The monthly DIC variations observed (ΔDIC_{obs}) in every box of the central North Sea and the calculated changes attributable to advection (ΔDIC_{adv}), air–sea exchange ($\Delta DIC_{air-sea}$), and biology (ΔDIC_{bio}).

		DIC (mmol C m^{-3} $month^{-1}$)											
Box		Jan	Feb	Mar	Apr	May	Jun	Jul	Aug	Sep	Oct	Nov	Dec
4	ΔDIC_{obs}	8	−13	−13	−13	−11	−11	−11	16	17	16	8	9
	ΔDIC_{adv}	0	−3	−2	−1	0	1	3	4	4	4	4	2
	$\Delta DIC_{air-sea}$	1	0	8	7	13	12	5	4	9	8	2	1
	ΔDIC_{bio}	8	−11	−20	−20	−24	−25	−19	9	4	4	1	5
14	ΔDIC_{obs}	1	1	1	1	8	8	8	−10	−9	−10	−1	0
	ΔDIC_{adv}	0	0	−1	−1	−2	−3	−4	−5	−3	−2	−1	−1
	ΔDIC_{bio}	1	1	2	3	10	11	12	−5	−6	−7	2	1
5	ΔDIC_{obs}	10	−13	−13	−13	−3	−3	−3	5	5	6	11	11
	ΔDIC_{adv}	2	2	2	2	2	2	1	1	2	2	2	2
	$\Delta DIC_{air-sea}$	0	−2	4	6	8	6	2	−1	−1	1	3	1
	ΔDIC_{bio}	8	−14	−20	−21	−13	−11	−6	4	5	3	6	8
15	ΔDIC_{obs}	10	−7	−7	−8	0	1	0	−3	−3	−3	10	10
	ΔDIC_{adv}	1	1	0	0	−1	−1	−2	−2	−1	0	0	0
	ΔDIC_{bio}	9	−8	−7	−8	1	2	2	−1	−2	−3	10	10

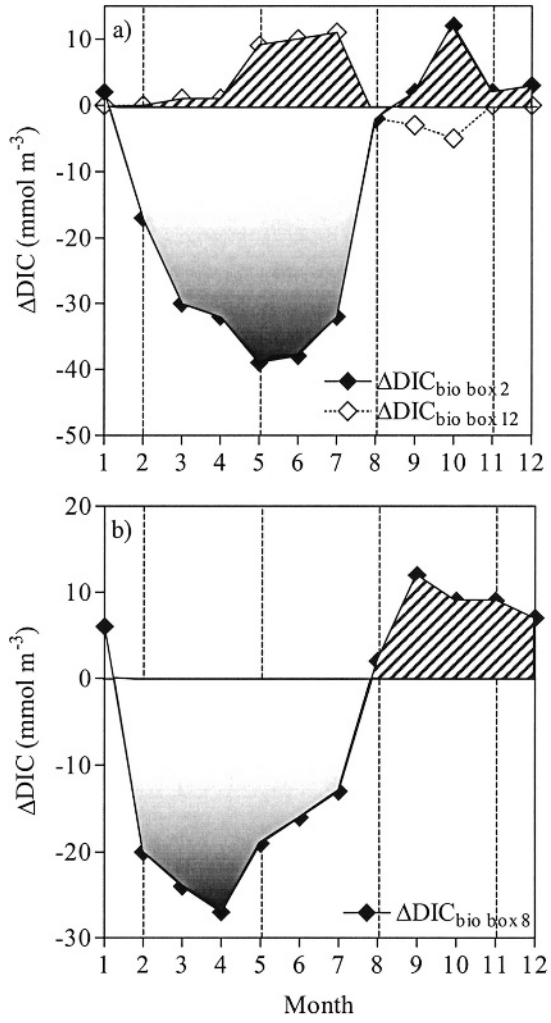

Fig. 6. Effect of the biology term (ΔDIC_{bio}) on DIC variation in (a) stratified boxes 2 and 12 and (b) the one-layer box 8. The negative integration area represents the period when GPP > R and governs the DIC variations in boxes 2 and 8 (i.e., positive NCP causes a decrease in DIC). The positive integration area represents the period when R > GPP and governs the DIC variations in boxes 12 and 8 (i.e., negative NCP causes an increase in DIC).

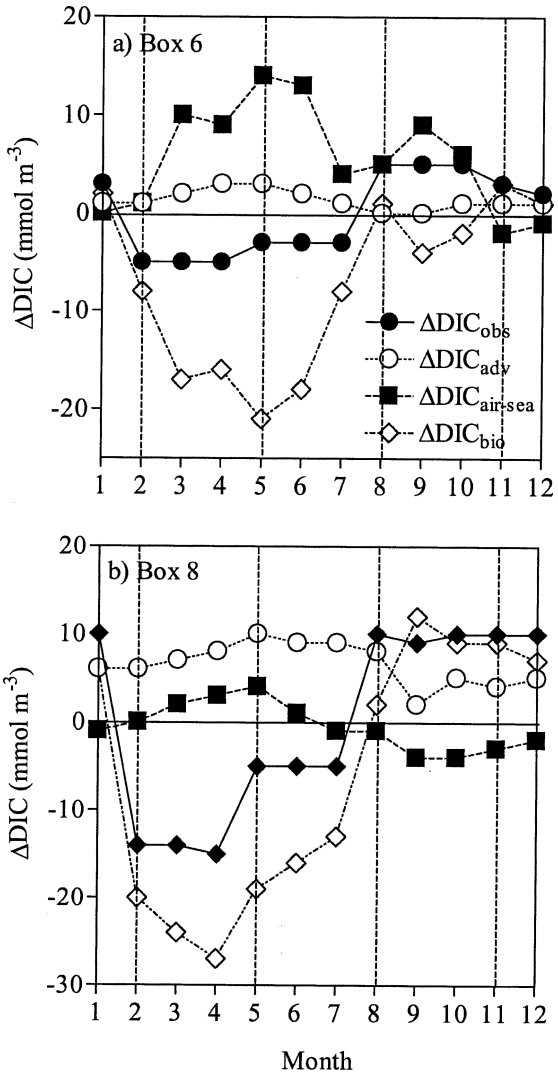

Fig. 7. Monthly effects of advection (ΔDIC_{adv}), air–sea CO_2 exchange ($\Delta DIC_{air-sea}$), and biological processes (ΔDIC_{bio}) on the variations of DIC (ΔDIC_{obs}) in the one-layer boxes 6 (a) and 8 (b).

with positive values of NCP_C ranging from a neutral trophic state to a maximum of 1.4 mol C m^{-2} $month^{-1}$ in May (Fig. 8a). The NCP_C calculated for this productive period in the upper layer of region 1 was 4.6 mol C m^{-2} (Table 7). For the rest of the year, NCP_C values were close to zero in all these surface boxes because GPP and R canceled each other out. In box 3, ERSEM overestimates the Baltic Sea water net inflow (Table 1) by a factor of three to four because of inadequate parameterization of the surface water level for the Baltic Sea (Thomas et al. 2005*a*). We corrected this valued using the net Baltic Sea carbon input given by Thomas et al. (2005*a*). This correction induces a larger error in ΔDIC_{adv} for the August–December period in this box, which results in positive NCP_C even though phytoplankton activity is not significant in the northern North Sea at this time of the year (Reid et al. 1990). The higher NCP_C calculated in box 3 seem to be an artifact of the larger advection term. The physical and chemical parameters measured during our fall and winter cruises showed similar properties in the surface waters of the northern North Sea (Tables 2, 3; Thomas 2002) because of the succession of strong wind events, which induce strong vertical and lateral mixing (Lenhart et al. 1995). On the basis of the homogeneity of the surface water of the North Sea, we can assume that NCP_C in box 3 (adjacent to boxes 1 and 2, in which NCP_C was insignificant) was insignificant at that time of the year. On the basis of this assumption, the annual NCP_C in the surface water of the North Sea was 4.9 mol C m^{-2} yr^{-1} (Table 7).

The deeper boxes of region 1 were clearly heterotrophic. NCP_C values ranged from a neutral trophic state to −5.4 mol C m^{-2} $month^{-1}$, with a minimum observed from April to July in boxes 11, 12, and 13 (Fig. 8b). For the entire year, NCP_C for the deeper layers of region 1 was −6.6 mol C m^{-2} yr^{-1} (Table 7).

Table 6. The monthly DIC variations observed (ΔDIC_{obs}) in every one-layer box of the southern North Sea and the calculated changes as a result of advection (ΔDIC_{adv}), air–sea exchange ($\Delta DIC_{air-sea}$), and biology (ΔDIC_{bio}).

		DIC (mmol C m^{-3} $month^{-1}$)											
Box		Jan	Feb	Mar	Apr	May	Jun	Jul	Aug	Sep	Oct	Nov	Dec
6	ΔDIC_{obs}	3	−5	−5	−5	−3	−3	−3	5	5	5	3	2
	ΔDIC_{adv}	1	1	2	3	3	2	1	0	0	1	1	1
	$\Delta DIC_{air-sea}$	0	1	10	9	14	13	4	5	9	6	−2	−1
	ΔDIC_{bio}	2	−8	−17	−16	−21	−18	−8	1	−4	−2	3	1
7	ΔDIC_{obs}	15	−13	−13	−12	−3	−3	−3	1	1	1	15	15
	ΔDIC_{adv}	3	1	3	4	6	6	6	7	7	7	8	6
	$\Delta DIC_{air-sea}$	−2	−2	1	2	3	1	0	−1	−3	−4	−3	−2
	ΔDIC_{bio}	14	−12	−17	−18	−11	−10	−9	−5	−38	−3	10	12
8	ΔDIC_{obs}	10	−14	−14	−15	−5	−5	−5	10	9	10	10	10
	ΔDIC_{adv}	6	6	7	8	10	9	9	8	2	5	4	5
	$\Delta DIC_{air-sea}$	−1	0	2	3	4	1	−1	−1	−4	−4	−3	−2
	ΔDIC_{bio}	6	−20	−24	−27	−19	−16	−13	2	12	9	9	7
9	ΔDIC_{obs}	10	−26	−26	−26	4	4	4	13	12	12	10	10
	ΔDIC_{adv}	−5	−5	−1	2	6	4	2	0	−2	−3	−5	−5
	$\Delta DIC_{air-sea}$	0	−2	4	5	7	5	1	−1	−2	−1	1	0
	ΔDIC_{bio}	15	−20	−29	−34	−9	−4	1	13	16	16	13	14
10	ΔDIC_{obs}	15	−12	−12	−12	−5	−5	−5	2	2	2	15	14
	ΔDIC_{adv}	15	5	0	−5	−9	−8	−7	−6	—	—	—	—
	$\Delta DIC_{air-sea}$	2	0	8	7	11	10	5	2	7	10	6	3
	ΔDIC_{bio}	−2	−17	−20	−14	−7	−7	−3	6	—	—	—	—

For the February–July period, region 2 was autotrophic with NCP_C values ranging from a neutral trophic state to 1.2 mol C m^{-2} $month^{-1}$ (Fig. 8c). In the deepest box 6, the NCP_C values were in the same range as in the north, with a maximum in May of 1.5 mol C m^{-2} $month^{-1}$. For that period, the NCP_C in region 2 was 4.5 mol C m^{-2}, which is similar to the value of 4.6 mol C m^{-2} calculated in the surface waters of region 1 during the same period (Table 7). However, because GPP is much higher in this area than in the northern area (Joint and Pomroy 1993; Moll 1997), these results show that high R occurs during the productive period in region 2. For the August–January period, region 2 was heterotrophic, characterized by NCP_C values ranging between −0.3 and −1.0 mol C m^{-2} $month^{-1}$. Integrated over the year, NCP_C is lower than in region 1, with a value of 3.1 mol C m^{-2} yr^{-1} (Table 7).

Discussion

NCP is commonly computed from nitrate or phosphate uptake and converted to carbon units with the Redfield ratio C : N : P = 106 : 16 : 1 (Redfield et al. 1963). This method is reliable when nitrate and phosphate are not depleted because DIC, nitrate, and phosphate are then consumed in the Redfield proportions (Arrigo 2005). However, it has long been recognized that conditions exist under which phytoplankton stoichiometry diverges from the canonical Redfield ratios (Droop 1973; Azam et al. 1983; Arrigo 2005). Thus, these ratios are not always, and not necessarily, appropriate to use to infer NCP from nitrate or phosphate fluxes, particularly in regions in which NCP has been observed during periods with depleted nitrate and phosphate in surface waters (Bégovic and Copin Montégut 2002; Falck and Anderson 2005; Kaltin and Anderson 2005). In the southern North Sea, the rivers and the atmosphere supply nitrate and phosphate continuously to the system, and the surface waters are never depleted throughout the year (Brockmann et al. 1990). In the northern North Sea, these inputs are not sufficient to maintain a background concentration of nitrate and phosphate, and the surface waters are depleted during late summer (Brockmann et al. 1990; Table 2). Therefore, the North Sea comprises two fundamentally different biogeochemical regions, where we can compare our NCP_C from our comprehensive DIC dataset with estimates of NCP on the basis of phosphate (NCP_P) and nitrate (NCP_N).

In the North Sea, previous investigations of NCP were based on such computations (Kempe and Pegler 1991; Helder et al. 1996; Smith et al. 1997). Smith et al. (1997) calculated, from a dissolved inorganic phosphate (DIP) mass balance approach, NCP in the areas between 51°N and 54°N and between 54°N and 57°N. On one hand, for the area between 51°N and 54°N, the monthly variations observed by Smith et al. (1997) follow the same trend as our results, with positive values of NCP from February to August and negative values from September to January. For this area, these authors report NCP values for the February–July period ranging from 0.5 (in February) to 0.2 mol C m^{-2} $month^{-1}$ (in August), with a maximum of 1.2 mol C m^{-2} $month^{-1}$ in April–May. These results are in good agreement with our monthly NCP_C values in the coastal boxes between 51°N and 54°N (Fig. 8c). The good agreement between these two calculations, one from DIC and the other from DIP, shows that these two parameters are consumed in Redfield proportions because phosphorus (and also nitrogen) is available during the entire productive period. In this case, the NCP is equivalent to new primary

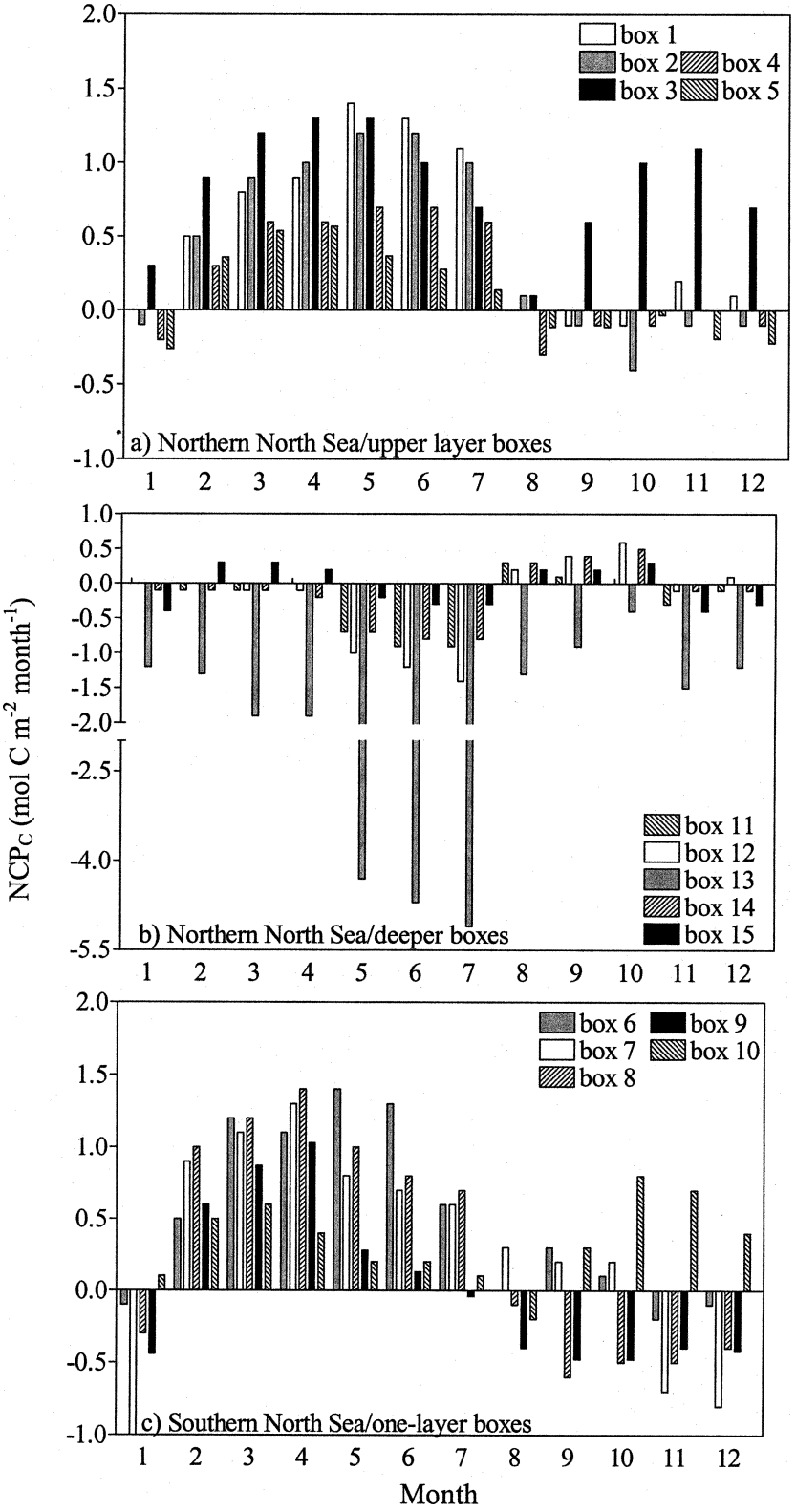

Fig. 8. Monthly net community production calculated from DIC data (NCP_C) in the (a) upper layer boxes (1–5), (b) deeper boxes (11–15), and (c) one-layer boxes (6–10). For the upper boxes, the NCP_C was calculated for the top 30 m of the water column. For the bottom boxes, the NCP_C was calculated from 30 m to the seafloor. For the one-layer boxes, the NCP_C was calculated for the maximum depth.

Table 7. Net community production for the February–July period and the whole year calculated for each surface ICES box, the upper layer of the northern North Sea, the area covered by the one-layer boxes, the area covered by all the deeper boxes, the area between 51°N and 57°N previously investigated by Smith et al. (1997), the upper layer of the entire North Sea, and the complete North Sea. NCP_C values are based on DIC, whereas NCP_N values are based on NO_x data and were converted to carbon units with the Redfield C : N ratio of 6.6. NCP_P values are based on the phosphate data measured during our cruises for the area between 51°N and 57°N and were converted to C units with a C : P ratio of 106 : 1. NCP_P^* is the value found by Smith et al. (1997) for this area. For the upper layer boxes, the DIC, NO_x, and PO_4^{3-} uptakes have been integrated over the first 30 m of the water column, whereas for the one-layer boxes, they have been integrated on the whole water column along the maximum depth of each box.

	February–July (mol C m^{-2})		Annual (mol C m^{-2} yr^{-1})	
Box	NCP_C	NCP_N	NCP_C	NCP_N
1	6.0	3.3	6.2	3.1
2	5.7	3.3	5.1	2.5
3	6.5	1.3	10.3	1.6
4	3.5	1.7	2.6	1.3
5	2.2	2.1	1.3	1.9
6	6.1	3.9	6.0	2.5
7	5.0	4.7	3.0	2.2
8	6.0	5.2	3.7	2.2
9	3.8	4.7	0.3	0.1
10	2.7	4.0	5.4	4.0
Upper boxes (1–5)	4.6	2.2	4.9	2.0
One-layer boxes (6–10)	4.5	4.7	3.1	0.8
Deeper boxes (11–15)	−5.7	—	−6.6	—
51–57°N	—	—	2.1	0.6 (NCP_P = 0.5)
Smith et al. (1997)	—	—	—	(NCP_P^* = 0.4)
North Sea upper layer	4.6	3.1	4.3	1.6
North Sea all	0.8	—	−0.1	—

production as defined by Dugdale and Goering (1967). On the other hand, in the stratified part of the North Sea between 54°N and 57°N, our monthly NCP_C were systematically higher than values calculated by Smith et al. (1997) from April to August, suggesting that DIC was consumed after the nutrient had been depleted. To verify this result, we computed net nitrogen consumption and converted it to NCP in carbon units (NCP_N) with the Redfield ratio of 6.6 (Fig. 9). We applied the mass balance approach of DIC to NO_x measured during our four cruises in the North Sea. The air–sea exchange term was replaced in Eq. 2 by the atmospheric deposition term from De Leeuw et al. (2001). These authors calculated N deposition for each box of a 30 by 30 km^2 grid mesh, which allows us to make an estimate of the deposition for each ICES box.

For the surface waters of region 1, the monthly NCP_C and NCP_N values were similar from February to April (Fig. 9a,b). This corresponds to the period when the surface waters were not depleted in nitrate (Table 2; Brockmann et al. 1990). During the May–July period in the NO_x-depleted surface waters of region 1, DIC was consumed as shown by the negative correlation between the NCP_C to NCP_N ratio and the NO_x surface concentrations (Fig. 10). Table 7 shows that NCP_C was 4.6 mol C m^{-2} for the February–July period in the upper layer of region 1 and exceeded NCP_N by 2.4 mol C m^{-2}. Consequently, for the whole surface of the North Sea, the NCP_C of 4.3 mol C m^{-2} yr^{-1} was higher than the NCP_N of 1.6 mol C m^{-2} yr^{-1} (Table 3). Similarly, Bégovic and Copin Montégut (2002) showed that NCP_C exceed NCP_N by 1.5 to 3 mol C m^{-2} (with NCP_C values ranging between 4.3 and 7.8 mol C m^{-2} in 1998 and 1999, respectively) during the productive period in the central western Mediterranean Sea. In the Baltic Sea, Thomas et al. (1999) and Osterroht and Thomas (2000) showed that the NCP_C exceeds NCP_N by a factor of 1 to 2.5. Recently, Falck and Anderson (2005) found in the surface waters of the Norwegian Sea an export production of 5.2 mol C m^{-2} yr^{-1} on the basis of the DIC mass balance budget, which corresponds to an excess consumption of carbon of 3.7 mol C m^{-2} yr^{-1} compared with the calculation on the basis of nitrogen. Our NCP_C estimates for the surface waters of the northern North Sea are within the range of values in these temperate seas. Similar to these studies, inorganic carbon consumption continues after nitrate is depleted in the surface waters (Figs. 9, 10). We suggest that both cell-internal and cell-external processes can explain the enhance DIC fixation. Schoeman et al. (2005) showed that during *Phaeocystis* blooms, a phytoplankton species predominant in the North Sea, values above the classical Redfield ratio (C : N = 6.6) are reported for cells growing under conditions of nutrient limitation, with the highest C : N cell ratios (up to 20 or 30 for different colonies) recorded under low-nutrient but high-light conditions. These authors explained that deviation of the C : N ratios in *Phaeocystis* colonies can be attributed to the increase in production of the mucilaginous matrix (mainly polysaccharidic). Thus, DIC consumption occurs under nutrient-depleted and high-light conditions. Mykelstad (1988) showed that when nitrate and phosphate are depleted, diatoms (which are abundant in the North Sea) produce more glucan (=carbohydrates) and therefore continue consuming DIC, whereas they stop synthesizing proteins (rich in N and P atoms), leading to an increase of the cellular C : N ratio. Moreover, van den Meersche et al. (2004) examined the different phases of a phytoplankton bloom in the Randers Fjord, Denmark. These authors showed that during the first period of the bloom, nutrients were replete, and an algal bloom was observed, with carbon and nitrogen uptake occurring at a constant Redfield ratio. This would be equivalent to our February–April period in the northern North Sea and to the entire productive period in the southern North Sea. In the second phase, the exhaustion of dissolved inorganic nitrogen resulted in decoupling of carbon and nitrogen flows caused by unbalanced algal growth: The carbon cycle had a pattern similar to the bloom phase, whereas the nitrogen cycle showed the characteristics of a nutrient-limited ecosystem. Approximately 71% of this assimilated carbon added to the phytoplankton biomass, whereas the algal nitrogen uptake

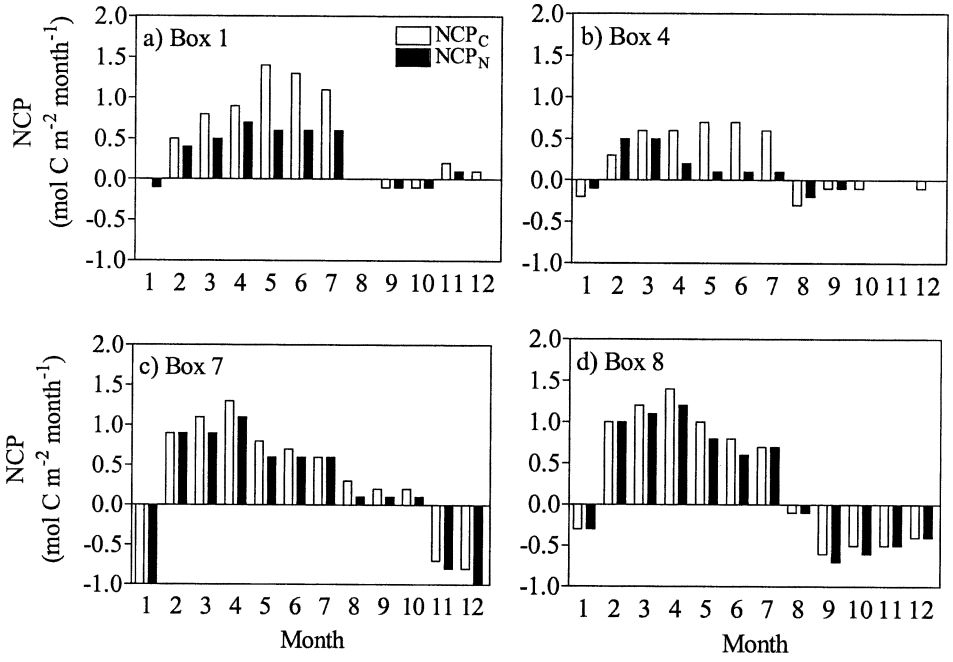

Fig. 9. Monthly net community production calculated from DIC (NCP_C) and NO_x (NCP_N) converted to carbon units with the Redfield ratio of 6.6 for two (a) northern and (b) central boxes as well as for (c, d) two southern boxes of the North Sea.

dropped to very low values, such that the algal nitrogen content decreased during this phase, resulting in high C : N ratios. This period corresponds to the May–August period when our NCP_C exceeded the NCP_N in the surface waters of region 1 (Fig. 10).

As far as cell-external processes are concerned, Azam et al. (1983) showed that the difference between NCP_C and NCP_N can be explained by preferential recycling of nitrate and phosphate during decaying blooms. Thus, new production by mainly pico- and nanoplankton is maintained with a cycling of nutrients, and DIC is used to a greater extend than nitrate and phosphate. The remaining carbon-enriched particulate organic matter is exported to the deeper water, as observed by Thomas et al. (1999) and Osterroht and Thomas (2000) in the Baltic Sea. This is in good agreement with results from Banse (1994), who showed that on disappearance of nitrate, DIC consumption can continue, resulting in a particulate organic carbon to particulate organic nitrogen ratio change to 13.6.

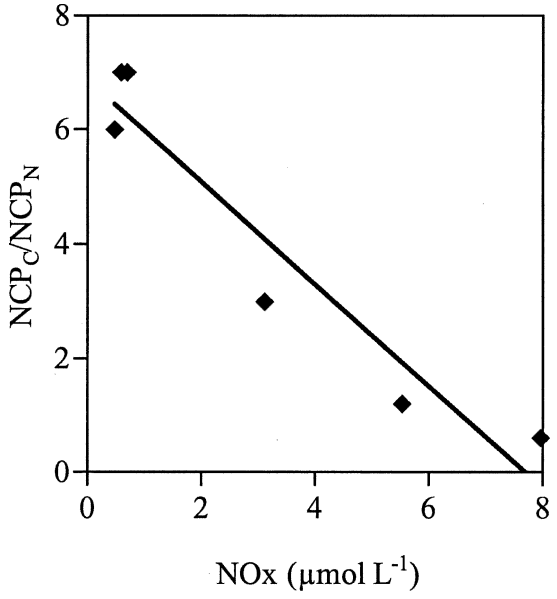

Fig. 10. Excess DIC uptake expressed as the $NCP_C : NCP_N$ ratio as a function of NO_x concentration during the productive period (February–July) in box 4. The linear regression yields $NCP_C/NCP_N = -0.89NO_x + 6.87$; $n = 6$, $r^2 = 0.91$.

To estimate the annual NCP in the entire 51°N–57°N region and compare it with the annual budget calculated by Smith et al. (1997) for the same area, we computed the annual NCP_C, NCP_N, and NCP_P (NCP from DIP) for the whole region. We found a NCP_P of 0.5 mol C m^{-2} yr^{-1} similar to their NCP_P value of 0.4 mol C m^{-2} yr^{-1} calculated for the same area for a different year. The ratio of consumption to respiration of phosphate appears to be constant from year to year. However, our NCP_C value of 2.1 mol C m^{-2} yr^{-1} is four- to fivefold higher than these NCP_P values and show that the net effect of biological production and respiration on the surface water inorganic carbon cannot be inferred from phosphate measurement by the Redfield ratio. We suggest that the discrepancies between the two values are mainly due to the consumption of DIC by the processes mentioned above in the central and northern North Sea, in which nitrate and phosphate are depleted during the April–August period. Moreover, our estimates of NCP_N and NCP_P of 0.6 and 0.5 mol C m^{-2} yr^{-1}, respectively (Table 7), are very close, revealing that the same processes drive the nitrate and phosphate cycles. Therefore, processes like nitrogen fixation, nitrifi-

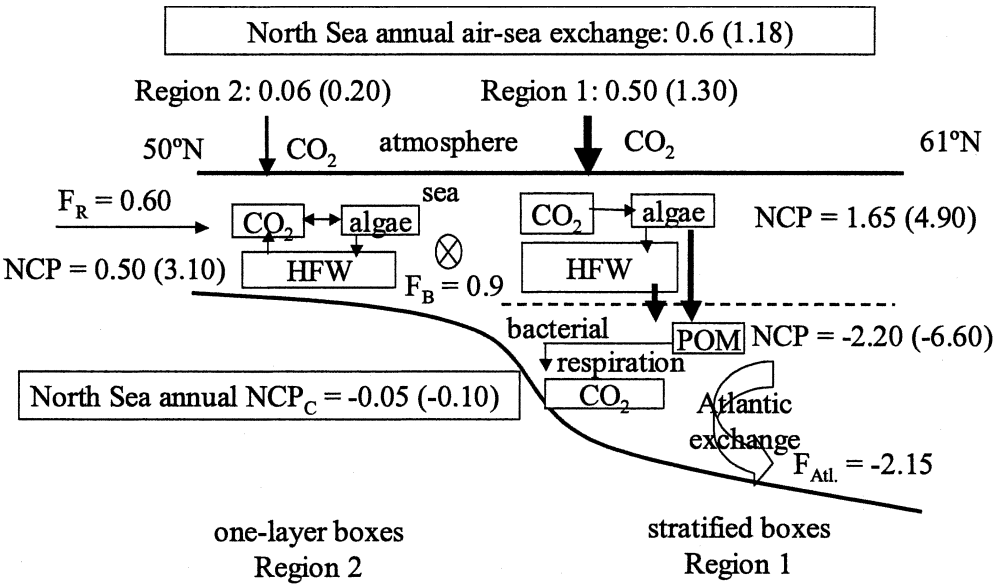

Fig. 11. Conceptual representation of inorganic carbon annual budget of the North Sea (expressed in 10^{12} mol C yr^{-1}; in parentheses, NCP_C and air–sea exchange numbers expressed in mol C m^{-2} yr^{-1}). Positive flows indicate inputs into the North Sea and negative ones outputs from the North Sea. The CO_2 air–sea fluxes in the upper panel were adapted from Thomas et al. (2004), and the river (F_R) and Baltic (F_B) inputs were adapted from Thomas et al. (2005*a*) for the surface area covered by the ICES boxes (513,004 km^2) for regions 1 and 2. In the bottom panel are indicated the NCP_C in regions 1 and 2 of the North Sea as well as for the entire study region. An estimate of the carbon transported from the North Sea to the North Atlantic Ocean ($F_{Atl.}$) is given in the bottom right panel.

cation or anammox, which are recognized for driving oceanic nutrients away from the Redfield ratios (Arrigo 2005) cannot be considered responsible for the discrepancies between NCP_C and NCP_N.

For region 2, the monthly calculated NCP_C and NCP_N followed a similar trend with similar values within the range of estimated error of 10% (Fig. 9c,d). In these areas, NO_x concentrations were never depleted and sustained net carbon production in the Redfield ratio proportions during the productive period (February–July), as observed in the first phase of a bloom by van den Meersche et al. (2004). The NCP_N is therefore equivalent to DIC consumption, with a value of 4.7 mol C m^{-2}, close to the NCP_C of 4.5 mol C m^{-2} (Table 7).

Recently, Thomas et al. (2005*b*) reported an independent evaluation of NCP in the North Sea on the basis of pCO_2 data measured in the same year as our DIC measurements. Their value of 4.3 mol C m^{-2} for NCP during the productive period, which according to these authors should be seen as a lower bound for the assessment of NCP, is in very good agreement with our value of 4.9 mol C m^{-2} from our DIC data set.

In the whole North Sea on an annual scale, production and consumption of organic matter balance each other with a NCP_C of -0.1 mol C m^{-2} yr^{-1}. This estimate is within the range of values derived from previous computations of -0.05 mol C m^{-2} yr^{-1} on the basis of organic carbon by Radach and Lenhart (1995) for the same area of 513,000 km^2. Moreover, a recent carbon budget provides evidence from both DIC and DOC observations that the North Sea is net heterotrophic with NCP of -0.5 ± 0.2 mol C m^{-2} yr^{-1} for an area of 575,300 km^2 (Thomas et al. 2005*a*), which is in a similar range as the results obtained in this study.

It is usually assumed that NCP accounts for 0.5% to 2% of the GPP in the North Sea (Helder et al. 1996; Smith et al. 1997), although highly variable. For the southern area, GPP values range between 6.6 and 21.7 mol C m^{-2} yr^{-1} in boxes 7 and 9, respectively (Joint and Pomroy 1993; Moll 1997), whereas they are close to 20.8 and 16.7 mol C m^{-2} yr^{-1} in the surface waters of the central and the northern North Sea, respectively (Joint and Pomroy 1993; Moll 1997). For the surface waters in the northern area, we calculated a NCP_C of 4.9 mol C m^{-2} yr^{-1} so that it might account for 20% to 30% of GPP. For the southern area, we calculated a NCP_C of $\sim$3.1 mol C m^{-2} yr^{-1}, which represents 15% of GPP of this area of the North Sea, an estimate higher than previous investigations.

Summary and conclusion

On the basis of a robust dataset of DIC, pCO_2, and related parameters covering every season during one year, combined with hydrodynamic data in the North Sea, we calculated the monthly variations of DIC resulting from abiotic and biological processes in the 15 ICES boxes.

During the December–February period in the surface layer of the northern and central North Sea, the DIC concentrations are very homogeneous because of advection and air–sea exchange of CO_2, which increase the DIC

content of the surface waters with values on the order of 0.4 and 0.2 mmol C m^{-2} $month^{-1}$, respectively, throughout that period. From February to July, NCP_C is the main factor driving the DIC variations in the surface waters of the North Sea, with values ranging from 0.5 to 1.4 mol C m^{-2} $month^{-1}$. Our calculation shows that most of the organic carbon produced during this period in the surface waters of the northern North Sea is then remineralized from April to July in the bottom layers, with values of NCP_C ranging from -0.5 to -5.5 mol C m^{-2} $month^{-1}$. From August to January in the shallow southern North Sea, biological processes govern the DIC variation, with NCP_C values ranging from -0.5 to -0.8 mol C m^{-2} $month^{-1}$.

In the surface layer, we calculated an annual NCP on the basis of DIC of 4.3 $\pm$ 0.4 mol C m^{-2} yr^{-1}, whereas NCP from nitrate was 1.6 $\pm$ 0.2 mol C m^{-2} yr^{-1}. We suggest that a combination of both extracellular and intracellular mechanisms occurring during the phase of a bloom when nutrients are depleted is responsible for this discrepancy. Extracellular recycling of nutrients and intracellular adaptation to the depleted nitrate and phosphate conditions observed for phytoplankton species abundant in the North Sea permit a consumption of DIC without major nutrients, which diverges from a balanced growth (in the Redfield sense) during these period.

The estimates of NCP_C for the different regions of the North Sea allow us to assess the role of biological activity in the efficiency of its continental shelf pump. Thomas et al. (2004) and Bozec et al. (2005) showed that the stratification of the water column in the northern North Sea during summer and the export of water to the North Atlantic Ocean were the main physical processes responsible for the efficient uptake of CO_2. The biological and physical processes driving this pump are shown in Fig. 11. The biological uptake of DIC of 1.65×10^{12} mol C yr^{-1} in the upper layer of region 1 allows an uptake of CO_2 from the atmosphere of 0.50×10^{12} mol C yr^{-1}. In region 2, although NCP_C is 0.50×10^{12} mol C yr^{-1}, the uptake from the atmosphere is smaller (0.06×10^{12} mol C yr^{-1}). This is because other parameters, such as temperature, drive the pCO_2 changes (Thomas et al. 2005*b*). The efficiency of the pump then relies on the combination of three processes: (1) strong stratification of the water column in region 1, which allows (2) the release of DIC ($NCP_C = -2.20 \times 10^{12}$ mol C yr^{-1}) consumed in the upper layer into the underlying deeper layer, thus avoiding degassing of CO_2 to the atmosphere, and (3) the transport of this DIC-enriched water mass to the deep waters of the adjacent North Atlantic Ocean (Fig. 11).

References

Arrigo, K. R. 2005. Marine microorganisms and global nutrient cycles. Nature **437:** 349–355.

Azam, F., T. Fenchel, J. G. Field, J. S. Gray, L. A. Meyerreil, and F. Thingstad. 1983. The ecological role of water-column microbes in the sea. Mar. Ecol. Prog. Ser. **10:** 257–263.

Banse, K. 1994. Uptake of inorganic carbon and nitrate by marine plankton and the Redfield ratio. Glob. Biogeochem. Cycles **8:** 81–84.

Bégovic, M., and C. Copin Montégut. 2002. Processes controlling annual variations in the partial pressure of CO_2 in surface waters of the central northwestern Mediterranean Sea (Dyfamed site). Deep-Sea Res. II **49:** 2031–2047.

Borges, A. V. 2005. Do we have enough pieces of the jigsaw to integrate CO_2 fluxes in the Coastal Ocean? Estuaries **28:** 3–27.

———, B. Delille, and M. Frankignoulle. 2005. Budgeting sinks and sources of CO_2 in the coastal ocean: Diversity of ecosystems counts. Geophys. Res. Lett. **32:** L14601. [doi:10.1029/2005GL023053]

Bozec, Y., H. Thomas, K. Elkalay, and H. J. W. De Baar. 2005. The continental shelf pump in the North Sea—evidence from summer observations. Mar. Chem. **83:** 131–147.

Brockmann, U. H., R. W. P. M. Laane, and H. Postma. 1990. Cycling of nutrient elements in the North Sea. Neth. J. Sea Res. **26:** 239–264.

Chen, C.-T. A. 2004. Exchange of carbon in the coastal seas, p. 341–351. *In* C. B. Field [ed.], The global carbon cycle: Integrating human, climate and the natural world. SCOPE, ISSN.

de Haas, H., T. C. E. Van Weering, and H. De Stigter. 2002. Organic carbon in shelf seas: Sinks or sources, processes and products. Cont. Shelf Res. **22:** 691–717.

De Leeuw, G., L. Cohen, L. M. Frohn, and others. 2001. Atmospheric input of nitrogen into the North Sea: ANICE project overview. Cont. Shelf Res. **21:** 2073–2094.

Droop, M. R. 1973. Some thoughts on nutrient limitation in algae. J. Phycol. **9:** 264–272.

Dugdale, R. C., and J. J. Goering. 1967. Uptake of new and regenerated forms of nitrogen in primary productivity. Limnol. Oceanogr. **12:** 196–206.

Falck, E., and L. G. Anderson. 2005. The dynamics of the carbon cycle in the surface water of the Norwegian Sea. Mar. Chem. **94:** 43–53.

———, and H. G. Gade. 1999. Net community production and oxygen fluxes in the Nordic Seas based on O_2 budget calculations. Glob. Biogeochem. Cycles **13:** 1117–1126.

Gattuso, J.-P., M. Frankignoulle, and R. Wollast. 1998. Carbon and carbonate metabolism in coastal aquatic ecosystems. Annu. Rev. Ecol. Syst. **29:** 405–434.

Gazeau, F., C. M. Duarte, J.-P. Gattuso, and others. 2005*a*. Whole system metabolism and CO_2 fluxes in a Mediterranean bay dominated by seagrass beds (Palma Bay, NW Mediterranean). Biogeosciences **2:** 43–60.

———, J.-P. Gattuso, J. J. Middelburg, N. Brion, L.-S. Schiettecatte, M. Frankignoulle, and A. V. Borges. 2005*b*. Planktonic and whole system metabolism in a nutrient-rich estuary (the Scheldt estuary). Estuaries **28:** 868–883.

Grasshoff, K., M. Ehrhardt, and K. Kremling. 1983. Methods of seawater analysis, 2nd ed. Verlag Chemie.

Helder, W., C. Schrum, and G. Shimmield. 1996. North Sea budget, p. 13–20. *In* J. Hall, S. V. Smith and P. R. Boudreau [eds.], Report on the International Workshop on Continental Shelf Fluxes of Carbon, Nitrogen and Phosphorus. LOICZ/R&S/96–9. LOICZ Core Project.

Holm-Hansen, O., C. J. Lorenzen, R. W. Homes, and J. D. H. Strickland. 1965. Fluorometric determination of chlorophyll. J. Cons. Explor. Mer. **30:** 3–15.

[ICES] International Council for the Exploration of the Sea. 1983. Flushing times of the North Sea. ICES Cooperative Research Report 123.

Joint, I., and A. Pomroy. 1993. Phytoplankton biomass and production in the southern North Sea. Mar. Ecol. Prog. Ser. **99:** 169–182.

KALTIN, S., AND L. G. ANDERSON. 2005. Uptake of atmospheric carbon dioxide in the Arctic seas: Evaluation of the relative importance of processes that influence pCO_2 in water transported over the Bering–Chukchi Sea shelf. Mar. Chem. **94:** 67–79.

KEMPE, S., AND K. PEGLER. 1991. Sinks and sources of CO_2 in coastal seas: The North Sea. Tellus **43B:** 224–235.

LENHART, H., AND T. POHLMANN. 1997. The ICES-boxes approach in relation to results of a North Sea circulation model. Tellus **49A:** 139–160.

LENHART, H. J., G. RADACH, J. O. BACKHAUS, AND T. POHLMANN. 1995. Simulations of the North Sea circulation, its variability, and its implementation as hydrodynamical forcing in ERSEM. Neth. J. Sea Res. **33:** 271–299.

MACKENZIE, F. T., A. LERMAN, AND A. J. ANDERSSON. 2004. Past and present of sediment and carbon biogeochemical cycling models. Biogeosciences **1:** 11–32.

MOLL, A. 1997. Modeling primary production in the North Sea. Oceanography **10:** 24–26.

MULLER-KARGER, F. E., R. VARELA, R. THUNELL, R. LUERSSEN, H. CHUANMIN, AND J. J. WALSH. 2005. The importance of continental margins in the global carbon cycle. Geophys. Res. Lett. **32**, LO1602, [doi:10.1029/2004GL021346]

MYKELSTAD, S. M. 1988. Production, chemical structure, metabolism, and biological function of the (1–3)-linked, β-D-glucans in diatoms. Limnol. Oceanogr. **6:** 313–326.

NIGHTINGALE, P. D., G. MALIN, C. S. LAW, AND OTHERS. 2000. In situ evaluation of air–sea gas exchange parameterizations using novel conservative and volatile tracers. Glob. Biogeochem. Cycles **14:** 373–387.

ODUM, H. T. 1956. Primary production in flowing waters. Limnol. Oceanogr. **1:** 102–117.

OSTERROHT, C., AND H. THOMAS. 2000. New production enhanced by nutrient supply from non-Redfield remineralisation of freshly produced organic material. J. Mar. Syst. **25:** 33–46.

RADACH, G., AND H. J. LENHART. 1995. Nutrient dynamics in the North Sea: Fluxes and budgets in the water column derived from ERSEM. Neth. J. Sea Res. **33:** 301–335.

REDFIELD, A. C., B. H. KETCHUM, AND F. A. RICHARDS. 1963. The influence of organisms on the composition of sea-water, p. 26–77. *In* M. N. Hill [ed.], The sea. Interscience.

REID, P. C., C. LANCELOT, W. W. C. GIESKES, E. HAGMEIER, AND G. WEICHART. 1990. Phytoplankton of the North Sea and its dynamics: A review. Neth. J. Sea Res. **26:** 295–331.

SABINE, C. L., R. A. FEELY, N. GRUBER, AND OTHERS. 2004. The oceanic sink for anthropogenic CO_2. Science **305:** 367–371.

SCHOEMANN, V., S. BECQUEVORT, J. STEFELS, V. ROUSSEAU, AND C. LANCELOT. 2005. *Phaeocystis* blooms in the global ocean and their controlling mechanisms: A review. J. Sea Res. **53:** 43–66.

SMITH, S. V., P. R. BOUDREAU, AND P. RUARDIJ. 1997. N and P budget for the southern North Sea [Internet]. Publisher: LOICZ Core Project. [accessed 2005 January]. Available from http://data.ecology.su.se/MNODE/Europe/NorthSea/NORTHSEA.HTM

THOMAS, H. 2002. Shipboard report of the RV *Pelagia* cruises 64PE184, 64PE187, 64PE190 and 64PE195. R. Neth. Inst. Sea Res, 63 p.

———, Y. BOZEC, H. J. W. DE BAAR, AND OTHERS. 2005*a*. The carbon budget of the North Sea. Biogeosciences **2:** 87–96.

———, ———, K. ELKALAY, AND H. J. W. DE BAAR. 2004. Enhanced open ocean storage of CO_2 from shelf sea pumping. Science **304:** 1005–1008.

———, ———, ———, ———, A. V. BORGES, AND L.-S. SCHIETTECATTE. 2005*b*. Controls of the surface water partial pressure of the CO_2 in the North Sea. Biogeosciences **2:** 323–334.

———, V. ITTEKKOT, C. OSTERROHT, AND B. SCHNEIDER. 1999. Preferential recycling of nutrients—the ocean's way to increase new production and to pass nutrient limitation? Limnol. Oceanogr. **44:** 1999–2004.

———, AND B. SCHNEIDER. 1999. The seasonal cycle of carbon dioxide in the Baltic Sea surface waters. J. Mar. Syst. **22:** 53–67.

TYRELL, T., AND A. MERICO. 2004. *Emiliana huxleyi*: Bloom observations and the conditions that induce them, p. 75–97. *In* H. R. Thierstein and J. R. Young [eds.], Coccolithophores. From molecular processes to global impact. Springer.

VAN DEN MEERSCHE, K., J. J. MIDDELBURG, K. SOETAERT, P. VAN RIJSWIJK, H. T. S. BOSCHKER, AND C. H. R. HEIP. 2004. Carbon–nitrogen coupling and algal–bacterial interactions during an experimental bloom: Modeling a ^{13}C tracer experiment. Limnol. Oceanogr. **49:** 862–878.

WALSH, J. J. 1991. Importance of continental margins in the marine biogeochemical cycling of carbon and nitrogen. Nature **350:** 53–55.

WANNINKHOF, R. 1992. Relationship between wind speed and gas exchange over the ocean. J. Geophys. Res. **97:** 7373–7382.

———, AND W. R. MCGILLIS. 1999. A cubic relationship between air–sea CO_2 exchange and wind speed. Geophys. Res. Lett. **26:** 1889–1892.

Received: 8 March 2005
Accepted: 30 May 2006
Amended: 17 July 2006